A LOCAL POLYNOMIAL JUMP DETECTION ALGORITHM IN NONPARAMETRIC REGRESSION

Peihua Qiu
Biostatistics Program
The Ohio State University
M200 Starling Loving Hall
320 West 10th Avenue
Columbus, OH 43210-1240

Brian Yandell
Department of Statistics
University of Wisconsin - Madison
1210 West Dayton Street
Madison, WI 53706

Abstract

We suggest a one dimensional jump detection algorithm based on local polynomial fitting for jumps in regression functions (zero-order jumps) or jumps in derivatives (first-order or higher-order jumps). If jumps exist in the m-th order derivative of the underlying regression function, then an $(m+1)$ order polynomial is fitted in a neighborhood of each design point. We then characterize the jump information in the coefficients of the highest order terms of the fitted polynomials and suggest an algorithm for jump detection. This method is introduced briefly for the general set-up and then presented in detail for zero-order and first-order jumps. Several simulation examples are discussed. We apply this method to the Bombay (India) sea-level pressure data.

Key Words: Nonparametric jump regression model, Jump detection algorithm, Least squares line, Threshold value, Modification procedure, Image processing, Edge detection.

1 Introduction

Stock market prices often jump up or down under the influence of some important random events. Physiological response to stimuli can likewise jump after physical or chemical shocks. Regression functions with jumps may be more appropriate than continuous regression models for such data. The one dimensional (1-D) nonparametric jump regression model (NJRM) with jumps in the m-th derivative can be expressed as

$$Y_i = f(t_i) + \epsilon_i,\ i = 1, 2, \cdots, n, \tag{1.1}$$

$$f^{(m)}(t) = g(t) + \sum_{i=1}^{p} d_i I_{[s_i, s_{i+1})}(t), \tag{1.2}$$

with design points $0 \le t_1 < t_2 < \cdots < t_n \le 1$ and iid errors $\{\epsilon_i\}$ having mean zero and unknown variance σ^2. The m-th order derivative $f^{(m)}(t)$ of the regression function $f(t)$ consists of a continuous part $g(t)$ and p jumps at positions $\{s_i, i = 1, 2, \cdots, p\}$ with magnitudes $\{d_i - d_{i-1}, i = 1, 2, \cdots, p\}$. For convenience, let $d_0 = 0$ and $s_{p+1} = 1$. Zero-order jumps ($m = 0$) in the regression function itself correspond to the step edge in image processing. First-order jumps ($m = 1$) may exist in the first derivative of $f(t)$, related to the roof edge in image processing. For $m > 1$, the jumps in (1.2) are called higher-order. The objective of this paper is to develop an algorithm to detect the jumps of 1-D NJRM (1.1)-(1.2) from the noisy observations $\{Y_i, i = 1, 2, \cdots, n\}$.

Example 1.1 (Bombay sea-level pressure data) Figure 1.1 shows a sea-level presure data which was provided by Dr. Wilbur Spangler at National Center for Atmospheric Research (NCAR), Boulder, Colorado. The small dots represent the December sea-level pressures during 1921-1992 in Bombay, India. Shea et al. (1994) pointed out that "a discontinuity is clearly evident around 1960. ... Some procedure should be used to adjust for the continuity". By usng the procedure introduced in this paper, a jump is detected. The fitted model with this detected jump accommodated is shown in the plot by the solid curves. As a comparison, we plot the fitted model with the usual kernel smoothing method by the dotted curve. More explanation about this example is given in Section 4.3.

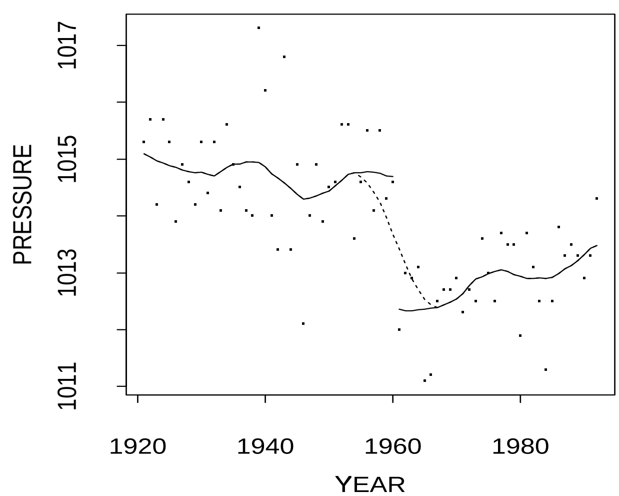

Figure 1.1: The December sea-level pressures during 1921-1992 in Bombay, India. The solid curves represent the fit from our jump-preserving algorithm. The dotted curve is the usual kernel smoothing fit without considering the jump structure.

McDonald and Owen (1986) proposed an algorithm based on three smoothed estimates of the regression function, corresponding to the observations on the right, left, and both sides of a point in question, respectively. They then constructed a "split linear smoother" as a weighted average of these three estimates, with weights determined by the goodness-of-fit values of the estimates. If there was a jump near the given point, then only some of these three estimates provided good fits, accommodating the discontinuities of the regression functions. Hall and Titterington (1992) suggested an alternative method by establishing some relations among three local linear smoothers and using them to detect the jumps. This latter method is easier to implement.

Related research on this topic includes kernel-type methods for jump detection in Müller (1992), Qiu (1991,1994), Qiu et al (1991), Wu and Chu (1993), Yin (1988), etc. These methods were based on the difference between two one-sided kernel smoothers. Wahba (1986), Shiau (1987) and several others regarded the NJRMs as partial linear regression models and fitted them with partial splines. More recently, Eubank and Speckman (1994) and Speckman (1993) treated the NJRM (1.1)-(1.2) as a semi-parametric regression model and proposed estimates of the jump locations and magnitudes. Loader (1994) suggested a jump detector based on local polynomial kernel estimators.

In this paper, we suggest an alternative method. At a given design point t_i, we consider its neighborhood $N(t_i) := \{t_{i-\ell}, t_{i+1-\ell}, \cdots, t_i, \cdots, t_{i-1+\ell}, t_{i+\ell}\}$ with width $k = 2\ell + 1 \ll n$ an odd positive integer, for $\ell + 1 \leq i \leq n - \ell$. We then fit a local polynomial function of order $(m+1)$ by the least squares (LS) method in that neighborhood, which can be expressed as

$$\hat{Y}^{(i)}(t) = \hat{\beta}_0^{(i)} + \hat{\beta}_1^{(i)} t + \cdots + \hat{\beta}_{m+1}^{(i)} t^{m+1}, t \in N(t_i), i = \ell + 1, \cdots, n - \ell. \tag{1.3}$$

Intuitively, if $f^{(m)}(t)$ is smooth at t_i, then $\hat{\beta}_{m+1}^{(i)}$ is close to $f^{(m+1)}(t_i)$ for large enough n. If $f^{(m)}(t)$ has a jump at t_i, however, $\{\hat{\beta}_{m+1}^{(j)}\}_{j=\ell+1}^{n-\ell}$ has an abrupt change at $\hat{\beta}_{m+1}^{(i)}$. Hence, these coefficients carry information about both the continuous and the jump components of $f^{(m)}(t)$ (given in (1.2)).

A jump detection criterion can be formed which excludes the information about the continuous part but preserves the jump information. An important feature of such algorithm is that it is easy to implement. From the above brief description, this algorithm is based on estimated LS coefficients which are available from all statistical softwares. Its computation complexity is $O(n)$. Another feature of this method is that it does not require the number of jumps to be known beforehand as most existing methods did. Jumps are automatically accommodated with our jump preserving curve fitting procedure.

We should point out that in our algorithm the window width k is still undefined. How should one choose a proper window width in practice ? This is a common problem in local smoothing methods. In some applications, people have used a visual intuitive method to adjust the window width. Hastie and Tibshirani (1987) suggested using 10-50% observations for each running lines smoother in their local scoring algorithm. Stone (1977) suggested the cross-validation method to choose the window width. For more discussions on the selection of the window width, please refer to Chapter 6 in Härdle (1991).

In most applications, we are interested in checking for jumps in the regression function itself or in its first-order derivative. Hence in the following sections, we concentrate on these two special cases. In Section 2, a jump detection criterion for the case of $m = 0$ is derived, with a corresponding algorithm. Jump detection in slope is discussed in Section 3. In Section 4, some simulation results are presented. We return to the Bombay (India) sea-level pressure data in Section 4.3. Our method is compared with some kernel-type methods in Section 5. We conclude the article with some remarks in Section 6. Some supporting materials are given in the Appendix.

At the end of this section, we want to point out that the 2-D version of the current problem (namely, jump detection in surfaces) is closely related to edge detection in image processing. We refer the interested readers to Besag *et al.* (1995), Gonzalez and Woods (1992), Qiu and Bhandarkar (1996), Qiu and Yandell (1997) and the references cited there.

2 Jump Detection in the Regression Functions

In this section we discuss the jump detection in the regression function itself. This corresponds to $m = 0$ in model (1.1)-(1.2). For simplicity of presentation, we assume that the design points are equally spaced over [0,1]. Most of the derivation of the jump detection criterion presented below is intuitive, although mathematically rigorous arguments are available. Based on the derived criterion, we suggest a jump detection algorithm at the end.

As we introduced in Section 1, we fit a least squares line

$$\hat{Y}^{(i)}(t) = \hat{\beta}_0^{(i)} + \hat{\beta}_1^{(i)} t, t \in N(t_i)$$

in a neighbourhood $N(t_i)$ at any design point t_i, for $\ell + 1 \leq i \leq n - \ell$. Throughout this paper we make the following assumption (AS1) on the NJRM of equations (1.1)-(1.2).

(AS1) Only one jump is possible in any neighbourhood $N(t_i)$. If t_i is a jump point, then no other jumps exist in $N(t_{i-k}) \cup N(t_i) \cup N(t_{i+k})$.

Remark 2.1 Assumption (AS1) implies that jump locations are not very close to each other. Alternatively, there is enough data (n large, k/n small) to distinguish nearby jumps. This assumption seems to be reasonable in many applications.

In Appendix A we present a theorem (Theorem A.1) which gives some properties of $\hat{\beta}_1^{(i)}$. By that theorem, $\hat{\beta}_1^{(i)} \sim B_1(t_i) := g'(t_i)$ when there is no jump in $N(t_i)$; and

$$\hat{\beta}_1^{(i)} \sim B_1(t_i) := g'_+(t_i) + h_1(r)C_0 - \gamma(r)C_1$$

if a jump exists in $N(t_i)$ and the jump location is at $t_{i-\ell+r}, 0 \leq r \leq 2\ell$, where "$\sim$" means that noise in the data and a high order term are ignored, C_0 and C_1 are the jump magnitudes of $f(t)$ and its first order derivative at the jump location, $\gamma(r)$ is a positive function taking values between 0 and 1, $h_1(r) := \frac{6nr}{k(k+1)}(1 - \frac{r}{k-1})C_0$ and $g'_+(t_i) = g'(t_i)$ if $r \neq \ell$.

Remark 2.2 We want to point out that some quantities used in this paper such as $k, \hat{\beta}_1^{(i)}$ and $h_1(r)$ all depend on n. We did not make this explicit in notations for simplicity. Their meaning should be clear from contexture introduction.

Example 2.1 Let $f(t) = 5t^2 + I_{[0.5,1]}(t)$. Consider a sample of size 100 and let k be 7. Then $\hat{\beta}_1^{(i)} \sim B_1(t_i) = 10t_i + I_{\{.47 \leq t_i \leq .53\}} \frac{6(.53-t_i)}{(.07)\cdot(.08)}(1 - \frac{.53-t_i}{.06}), 4 \leq i \leq 97$. $\{B_1(t_i), 4 \leq i \leq 97\}$ is shown in Figure 2.1(a).

From Figure 2.1(a) and Theorem A.1 in Appendix A, we can see that $\{\hat{\beta}_1^{(i)}\}$ carries useful information about the jumps. This information is mainly in the "jump factor" $h_1(r)C_0$ of $B_1(t_i)$. $h_1(r)$ has a maximum value at $r = \ell$ of $\frac{1.5n(k-1)}{k(k+1)} = O(n/k)$ which tends to infinity with n. If we have prior information about the bound of the "continuous factor" $g'(t_i)$ (in the case t_i is not a jump point), then those points could be flagged as jump points if their LS slopes are bigger than the prior bound. However, that prior bound may not be available in many applications. Our strategy to overcome this difficulty is to find an operator to remove the continuous factor from $B_1(t_i)$ and to preserve its jump factor at the same time. Notice that the continuous factors $g'(t_i)$ and $g'(t_j)$ are close to each other when t_i and t_j are close. Therefore, a difference-type operator can remove the continuous factor. When t_i and t_j are far enough apart such that only one of $B_1(t_i)$ and $B_1(t_j)$ can have a jump factor, the difference between $B_1(t_i)$ and $B_1(t_j)$ preserves the jump factor. Many

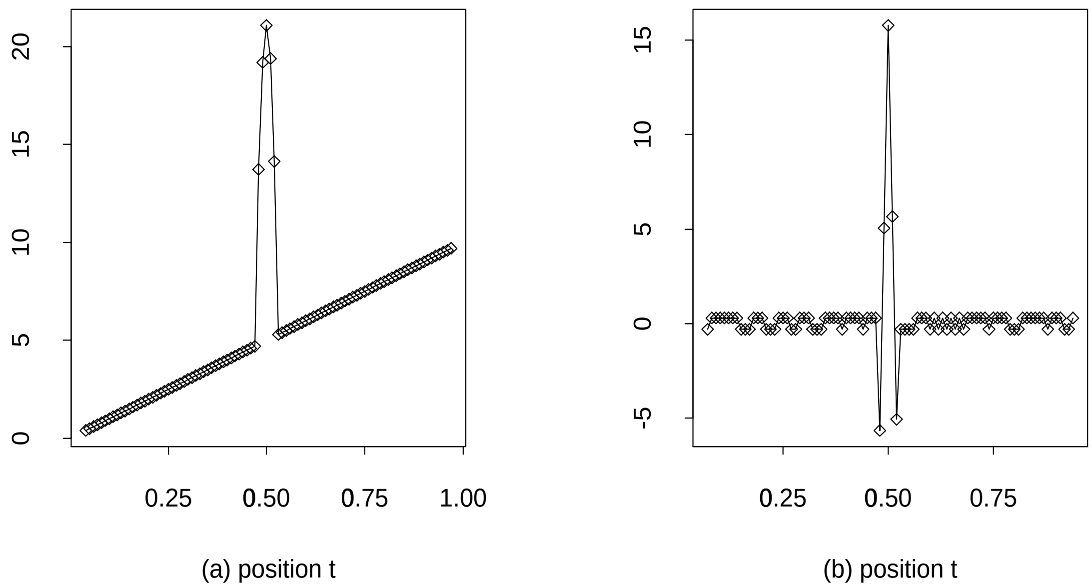

Figure 2.1: If $f(t) = 5t^2 + I_{[0.5,1]}(t)$, $n = 100, k = 7$, then $\hat{\beta}_1^{(i)} \sim B_1(t_i)$. $\{B_1(t_i)\}$ consists of both the continuous and the jump factors. It is shown in plot (a) by the "diamond" points. After using the difference operator defined in (2.1), $\{J_1(t_i)\}$ consists mainly of the jump factor. It is shown in plot (b).

difference-type operators could be found. In this paper, we suggest using the following:

$$\Delta_1^{(i)} := \begin{cases} \hat{\beta}_1^{(i)} - \hat{\beta}_1^{(i-\ell)} & \text{if } |\hat{\beta}_1^{(i)} - \hat{\beta}_1^{(i-\ell)}| \le |\hat{\beta}_1^{(i)} - \hat{\beta}_1^{(i+\ell)}| \\ \hat{\beta}_1^{(i)} - \hat{\beta}_1^{(i+\ell)} & \text{if } |\hat{\beta}_1^{(i)} - \hat{\beta}_1^{(i-\ell)}| > |\hat{\beta}_1^{(i)} - \hat{\beta}_1^{(i+\ell)}| \end{cases} \tag{2.1}$$

for $k \le i \le n-k+1$. That is, use the difference of smaller magnitude. By the above intuitive explanations, we can see that

$$\Delta_1^{(i)} \sim J_1(t_i) := \begin{cases} 0 & \text{if there is no jump in } N(t_i) \\ h_2(r)C_0 & \text{if there is a jump at } t_{i-\ell+r}, 0 \le r \le k-1 \end{cases} \tag{2.2}$$

where $h_2(r)$ is one of $h_1(r) - h_1(r-\ell)$ and $h_1(r) - h_1(r+\ell)$ with smaller magnitude and $h_1(j) = 0$ when $j < 0$ or $j > k-1$.

$h_2(r)$ has the same maximum value as $h_1(r)$. In the case of example 2.1, $\{J_1(t_i), 7 \le i \le 94\}$ is shown in Figure 2.1(b). From (2.2) and Figure 2.1(b), we can see that $\{\Delta_1^{(i)}\}$ does keep the jump information and delete the continuous factors at the same time. Hence it could be used as our jump detection criterion.

Remark 2.3 A possible alternative operator to (2.1) is as follows. For $k \leq i \leq n-k+1$, define

$$\Delta_*^{(i)} := \frac{|\hat{\beta}_1^{(i)} - \hat{\beta}_1^{(i+\ell)}|(\hat{\beta}_1^{(i)} - \hat{\beta}_1^{(i-\ell)}) + |\hat{\beta}_1^{(i)} - \hat{\beta}_1^{(i-\ell)}|(\hat{\beta}_1^{(i)} - \hat{\beta}_1^{(i+\ell)})}{|\hat{\beta}_1^{(i)} - \hat{\beta}_1^{(i-\ell)}| + |\hat{\beta}_1^{(i)} - \hat{\beta}_1^{(i+\ell)}|}$$

$\Delta_*^{(i)}$ is a weighted average of $\hat{\beta}_1^{(i)} - \hat{\beta}_1^{(i-\ell)}$ and $\hat{\beta}_1^{(i)} - \hat{\beta}_1^{(i+\ell)}$. From Theorem A.1 and Figure 2.1(a), we can check that $\Delta_*^{(i)}$ is small when there is no jump in $N(t_i)$. When there is a jump at t_i, $\Delta_*^{(i)} \sim h_1(\ell)C_0$ where C_0 is the jump magnitude.

Remark 2.4 The difference operator in (2.1) also narrows the regions that contain jump information. A jump affects $\hat{\beta}_1^{(i)}$ if t_i is within $2k$ of that jump point while it affects $\Delta_1^{(i)}$ when t_i is less than k units away. However, we also pay the price for that difference operator. The variance of $\Delta_1^{(i)}$ is usually bigger than the variance of $\hat{\beta}_1^{(i)}$. Although it does not affect much of the jump detection in the sense of large sample theory since both of them converge to zero, it might be important in finite sample cases. In applications, we suggest plotting both $\{\hat{\beta}_1^{(i)}\}$ and $\{\Delta_1^{(i)}\}$. In many cases the plot of $\{\hat{\beta}_1^{(i)}\}$ could be very helpful to demonstrate the jumps. This can be seen in the real data example (Section 4.3) and in the simulation examples (Sections 4.1 and 4.2) as well.

Large values of $|\Delta_1^{(i)}|$ indicate possible jumps near t_i. If there is no jump in $N(t_i)$, then $\hat{\beta}_1^{(i)} - \hat{\beta}_1^{(i-\ell)}$ is approximately normally distributed with mean zero, since it is a linear combination of the observations. From (2.1), $P(|\Delta_1^{(i)}| > u_{1i}) \leq P(|\hat{\beta}_1^{(i)} - \hat{\beta}_1^{(i-\ell)}| > u_{1i})$ for any $u_{1i} > 0$. Therefore consider the threshold value $u_{1i} = Z_{\alpha_n/2}\sigma^{(i)}$, with $\sigma^{(i)}$=SD of $\hat{\beta}_1^{(i)} - \hat{\beta}_1^{(i-\ell)}$. Clearly, $\sigma^{(i)}$ is independent of i. After some calculations, we have $\sigma^{(i)} = \frac{n}{k}\sqrt{\frac{6(5k-3)}{k^2-1}}\sigma$. Therefore a natural choice of the threshold value is

$$u_1 = \hat{\sigma} Z_{\alpha_n/2} \frac{n}{k}\sqrt{\frac{6(5k-3)}{k^2-1}}, \tag{2.3}$$

where $\hat{\sigma}$ is a consistent estimate of σ.

The design points $\{t_{i_j} : |\Delta_1^{(i_j)}| > u_1, j = 1, 2, \cdots, n_1\}$ can be flagged as candidate jump positions. If t_{i_j} is flagged, then its neighboring design points will be flagged with high probability. Therefore we need to cancel some of the candidates in $\{t_{i_j}, j = 1, 2, \cdots, n_1\}$. We do this by the following modification procedure which was first suggested by Qiu (1994).

Modification Procedure: For $\{t_{i_j}, j = 1, 2, \cdots, n_1\}$, if there are $r_1 < r_2$ such that the increments of the sequence $i_{r_1} < \cdots < i_{r_2}$ are all less than the window width k but $i_{r_1} - i_{r_1 - 1} > k$ and $i_{r_2+1} - i_{r_2} > k$, then we say that $\{t_{i_j}, j = r_1, r_1 + 1, \cdots, r_2\}$ forms a *tie* in $\{t_{i_j}, j = 1, 2, \cdots, n_1\}$. Select the middle point $(t_{i_{r_1}} + t_{i_{r_2}})/2$ for each tie as a jump position candidate, replacing the tie set in the candidate set $\{t_{i_j}, j = 1, 2, \cdots, n_1\}$. That is, reduce the candidate set to one representative, the middle point, from each tie set. After the above modification procedure, the present candidates include two types of points: those which do not belong to any tie, and the middle points of all of the ties.

The jump detection method is summarized in the following algorithm.

The Zero-order Jump Detection Algorithm:

1. *For any t_i, $\ell + 1 \leq i \leq n - \ell$, fit a least squares line in $N(t_i)$.*
2. *Use formula (2.1) to calculate $\Delta_1^{(i)}, k \leq i \leq n - k + 1$.*
3. *Use formula (2.3) to calculate the threshold value u_1.*
4. *Flag the design points $\{t_{i_j}, j = 1, 2, \cdots, n_1\}$ where t_{i_j} satisfies $|\Delta_1^{(i_j)}| > u_1$ for $j = 1, 2, \cdots, n_1$.*
5. *Use the modification procedure to determine the final candidates set $\{b_i, i = 1, 2, \cdots, q_1\}$. Then we conclude that jumps exist at $b_1 < b_2 < \cdots < b_{q_1}$.*

Remark 2.5 The least squares lines fitted in step 1 of the above algorithm can be updated easily from one design point to the next one, since only two points change. Thus the whole algorithm requires $O(n)$ computation. This remark is also true in the general set-up.

Remark 2.6 There is no difference for our jump detection whether we fit the model (1.3) or fit the centered model.

$$\hat{Y}^{(i)}(t) = \hat{\beta}_0^{(i)} + \hat{\beta}_1^{(i)}(t - t_i) + \cdots + \hat{\beta}_{m+1}^{(i)}(t - t_i)^{m+1}, t \in N(t_i), i = \ell + 1, \cdots, n - \ell$$

In many situations, it is more convenient to use the above model.

Theorem 2.1 Besides the conditions stated in Theorem A.1 in Appendix A, if the confidence level α_n in (2.3) satisfies the conditions that (i) $\lim_{n\to\infty} \alpha_n = 0$ (ii) $\lim_{n\to\infty} Z_{\alpha_n/2}/\sqrt{loglogk} = \infty$ and (iii) $\lim_{n\to\infty} Z_{\alpha_n/2}/\sqrt{k} = 0$, then (1) $\lim_{n\to\infty} q_1 = p$, $a.s.$; and (2) $\lim_{n\to\infty} b_i = s_i$, $a.s.$, $i = 1, 2, \cdots, p$. The rate of these convergences is $o(n^{-1}log(n))$.

(Proof is given in Appendix B.)

After we detect the possible jump locations $b_1 < b_2 < \cdots < b_{q_1}$, the regression function $f(t)$ could be fitted separately in intervals $\{(b_{i-1}, b_i), i = 1, 2, \cdots, q_1 + 1\}$ where $b_0 = 0$ and $b_{q_1+1} = 1$.

To fit $f(t)$ in each interval (b_{i-1}, b_i), we could use either global smoothing method (e.g., the smoothing spline method, Wahba, 1991) or local smoothing method (e.g., the kernel smoothing method, Härdle, 1991; the local polynomial kernel method, Wand and Jones, 1995). By using the kernel smoothing method, "boundary kernels" are necessary in the border regions of the intervials (see e.g., Stone, 1977). When $t \in (b_{i-1}, b_i)$, $\hat{f}(t)$ can be defined as follows.

$$\hat{f}(t) = \frac{\sum_{j=1}^{n} K_{ni}(t_j - t) y_j}{\sum_{j=1}^{n} K_{ni}(t_j - t)} \tag{2.4}$$

with $K_{ni}(x) = K(x/h_n) I_{\{t+x \in (b_{i-1}, b_i)\}}$ where $K(x)$ is a kernel function with $K(x) = 0$ when $x \notin [-1, 1]$ and h_n is a parameter related to the window size k by $h_n = \frac{k}{2n}$.

3 Jump Detection in Derivatives

Derivatives can be developed in an analogous manner. We consider only the jump detection in the first-order derivative for convenience. As we introduced in Section 1, we fit the following quadratic functions by the least squares method for jump detection.

$$\hat{Y}^{(i)}(t) = \hat{\beta}_0^{(i)} + \hat{\beta}_1^{(i)} t + \hat{\beta}_2^{(i)} t^2, t \in N(t_i), i = \ell + 1, \cdots, n - \ell$$

Theorem A.2 in Appendix A gives some properties of $\hat{\beta}_2^{(i)}$. It says that under some regularity conditions $\hat{\beta}_2^{(i)} \sim B_2(t_i) := g'(t_i)$ when there is no jump in $N(t_i)$, where $g(t)$ is the continuous part of $f'(t)$. When there is a jump in $N(t_i)$ and the jump location is at $t_{i-\ell+r}, 0 \le r \le 2\ell$, then

$$\hat{\beta}_2^{(i)} \sim B_2(t_i) := g'_+(t_i) + h_3(r) C_1 - \gamma(r) C_2$$

where C_1 and C_2 are jump magnitudes of $f'(t)$ and its first order derivative, $\gamma(r)$ is a positive function taking values in [0,1],

$$h_3(r) := \frac{r(k-1-r)k[(k-1)(k-2) - 3r(k-1-r)]}{12(k s_4 - s_2^2) n^3},$$

$s_p = \sum_{j=i-\ell}^{i+\ell} (t_j - t_i)^p$, $p = 2, 4$, and $g'_+(t_i) = g'(t_i)$ if $r \ne \ell$.

Example 3.1 Let $f'(t) = 5t^2 + I_{[0.5,1]}(t)$. Consider a sample of size 100 and let k be 11. Then $\hat{\beta}_2^{(i)} \sim B_2(t_i) = 10 t_i + I_{\{.45 \le t_i \le .55\}} h_3(100(.55 - t_i)), 6 \le i \le 95$. $\{B_2(t_i)\}$ is shown in Figure 3.1(a).

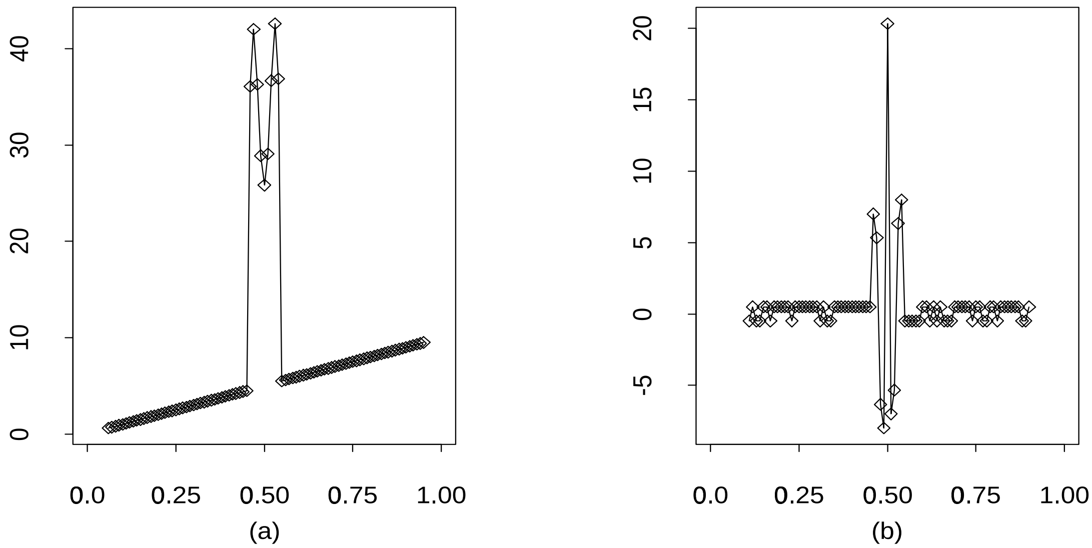

Figure 3.1: If $f'(t) = 5t^2 + I_{[0.5,1]}(t)$, $n = 100$, k is chosen to be 11, then $\hat{\beta}_2^{(i)} \sim B_2(t_i)$. $\{B_2(t_i)\}$ is shown in (a) by the "diamond" points. After using the difference operator which is similalar to that in (2.1)-(2.2), we get $\{J_2(t_i)\}$ which is shown in (b).

Similar to (2.1)-(2.2) in Section 2, we construct $\{\Delta_2^{(i)}\}$ from $\{\hat{\beta}_2^{(i)}\}$ and we have $\{J_2(t_i)\}$ which is shown in Figure 3.1(b) in the case of example 3.1. The threshold value for $\{\Delta_2^{(i)}\}$ is derived in the similar way to u_1, as

$$u_2 = \hat{\sigma} Z_{\alpha_n/2} \frac{\sqrt{k^2 s_4 - (k+1)s_2^2}}{k s_4 - s_2^2}. \tag{3.1}$$

The jump detection algorithm in Section 2 can be used here with $\{\Delta_2^{(i)}\}$ and u_2 substituting for $\{\Delta_1^{(i)}\}$ and u_1.

4 Numerical Examples

4.1 Jumps in Mean Response

We conducted some simulations using the example from Hall and Titterington (1992), which is shown in Figure 4.1. 512 observations $\{Y_i\}$ are obtained from $f(t_i)+\epsilon_i$ for equally spaced $t_i = i/512$, with errors from $N(0, \sigma^2)$ and $\sigma = 0.25$. The regression function $f(t) = 3 - 4t$ when $0 \le t \le 0.25$; $f(t) = 2 - 4t$ when $0.25 < t \le 0.5$; $f(t) = -1 + 4t$ when $0.5 < t \le 0.75$; $f(t) = 4 - 4t$ when $0.75 < t \le 1$. $f(t)$ has three jumps, at 0.25, 0.5 and 0.75, and corresponding jump magnitudes of -1,1 and -1, respectively.

We use the zero-order jump detection algorithm to detect the jumps, initially with $k = 31$. $\{\hat{\beta}_1^{(i)}\}$ is shown in Figure 4.2(a). According to the discussions in section 2, $\hat{\beta}_1^{(i)} \sim B_1(t_i)$, including a continuous factor and a jump factor. The jump factor has its effect only in the neighborhoods of the jump locations. The continuous factor is negative in intervals $0 \le t \le 0.25, 0.25 < t \le 0.5$ and $0.75 < t \le 1$ and positive in interval $0.5 < t \le 0.75$. All of these facts can be seen from Figure 4.2(a). We then use operator (2.1) to remove the continuous factors from $\{\hat{\beta}_1^{(i)}\}$. The remaining jump factors $\{\Delta_1^{(i)}\}$ are shown in Figure 4.2(b). From the graph, we can see that $\{\Delta_1^{(i)}\}$ waves around zero when t_i is not in the neighbourhoods of the jumps. This implies that the continuous factor is mostly removed. As we noticed in Remark 2.4, $\{\Delta_1^{(i)}\}$ seems noisier than $\{\hat{\beta}_1^{(i)}\}$. Figure 4.2(a) reveals the jumps very well in this case since the continuous factor does not contaminate much of the jump information. From the graphs we can approximate the jump positions and estimate the jump magnitudes from the relationship $M \sim h_2((k-1)/2)C_0 = \frac{1.5n(k-1)}{k(k+1)}C_0$, where M is the maximum/minimum value of $\{\Delta_1^{(i)}\}$ in the neighborhood of each of the detected jump positions and C_0 is the corresponding jump magnitude. For example, in Figure 4.2(b), we can see that there is a jump near 0.75 and M is about -23. Thus the jump magnitude C_0 is about $C_0 \approx [\frac{1.5n(k-1)}{k(k+1)}]^{-1} M \approx -0.99$.

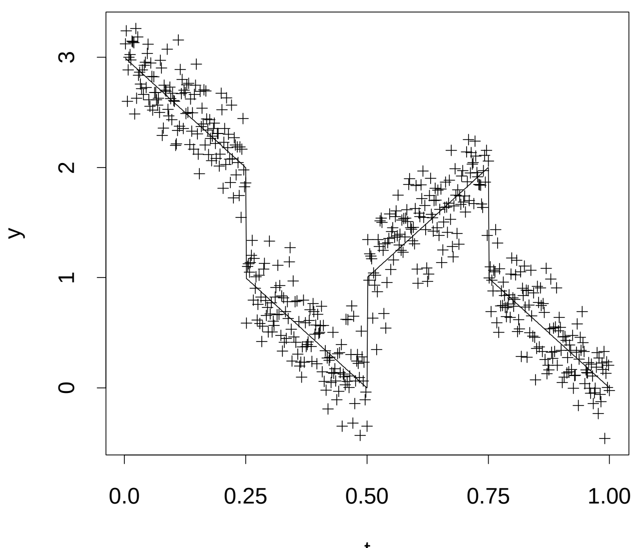

Figure 4.1: Hall and Titterington function f (solid lines) and observations (+).

As we noticed in Section 2, if the noise is not took into account, $\{\Delta_1^{(i)}\}$ has a peak with value $\frac{1.5n(k-1)}{k(k+1)}C_0$ at a jump point with jump magnitude C_0. Comparing with the threshold value in (2.3),

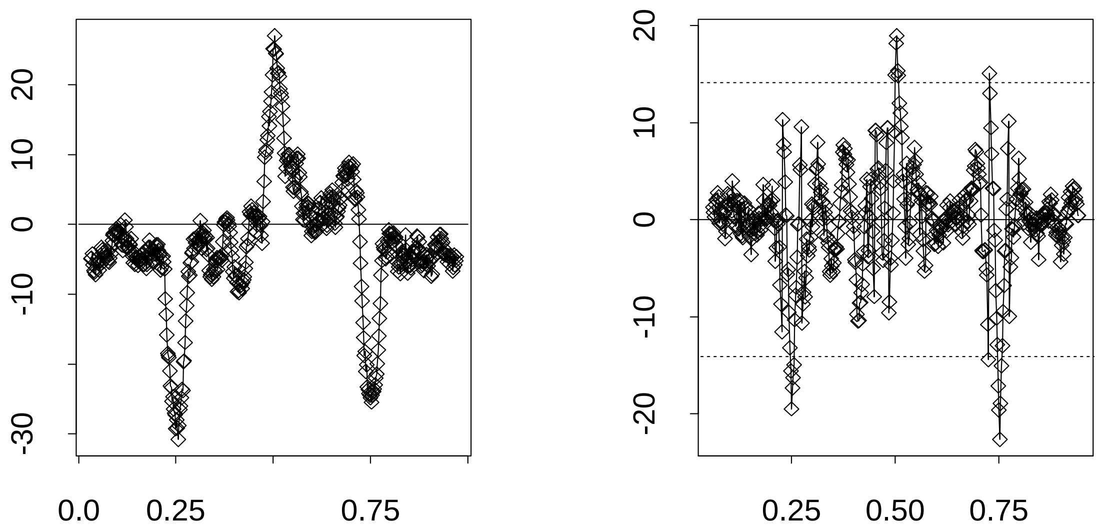

(a) (b)

Figure 4.2: (a) Slope estimates $\{\hat{\beta}_1^{(i)}\}$ (b) Jump information terms $\{\Delta_1^{(i)}\}$. The dotted lines in plot (b) indicate (+) or (−) threshold value u_1 corresponding to $Z_{\alpha_n/2} = 3.5$.

this jump could be detected if the jump magnitude satisfies

$$C_0 > \frac{\hat{\sigma} Z_{\alpha_n/2}(6(k+1)(5k-3))^{1/2}}{1.5(k-1)^{3/2}}. \tag{4.1}$$

Although n is not in (4.1), it is actually hidden in k since the above arguments are true only in the case that k/n is small and n is large. (4.1) tells us that (1) if σ is bigger (the data is noisier), then only jumps with larger jump magnitudes could be detected; (2) if the confidence level is set higher (α_n is small and $Z_{\alpha_n/2}$ is large), then the algorithm is more conservative (jumps with small jump magnitudes would probably be missed); (3) if k is larger (n is also larger), the algorithm could detect jumps with smaller magnitudes or could detect the same jumps with higher confidence level. This last point also implies that to detect the same jump the confidence level could be set a little bit higher when the sample size is larger.

In this simulation example, we use $n = 512$ and $k = 31$. The peak value of $\{\Delta_1^{(i)}\}$ is about 23.2258. The variance of $\{\Delta_1^{(i)}\}$ is less than 4.0245 (c.f. the derivation of (2.3)). We choose $Z_{\alpha_n/2} = 3.5$ in the threshold, which corresponds to $\alpha_n = 0.0004$. By (2.3), the threshold value is 14.08 which is smaller than the peak value more than 2 times the variance of $\{\Delta_1^{(i)}\}$. By (4.1), the algorithm could detect jumps with minimum jump magnitude about 0.6. If $k = 49$ which is the best width according to Table 4.1 introduced below, then this minimum magnitude could be decreased to about 0.47.

1000 independent trials were done, with 963 times to detect 3 jumps, 29 times to detect 2 jumps, 7 times to detect 4 jumps and 1 time to detect only 1 jump. The detected jump locations are shown in Figure 4.3.

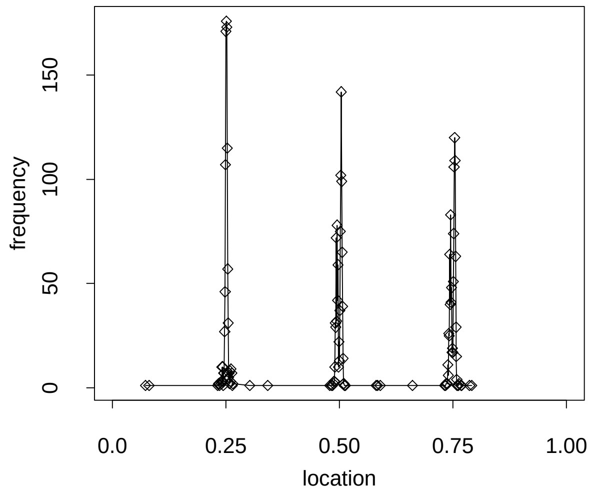

Figure 4.3: Frequency of detected jump locations by the zero-order jump detection algorithm with $n = 512$ and $k = 31$ for 1000 replications.

The choice of $k = 31$ is somewhat arbitrary. We investigated this with simulations for several n and k values. The results summarized in Figure 4.4 show that if k is chosen very small, some jumps are frequently missed, as the noise of $\Delta_1^{(i)}$ swamps the jump information. If k is very large, the wide window width makes the jump information be contaminated by the continuous factors. The corresponding results are not impressive either. The ratios of the "best" window widths (the smallest window widths that give the best results) to the sample sizes have the relations that $35/256 > 49/512 > 79/1024 > 145/2048$. This suggests that the ratio of the window size to the sample size should be decreasing as n increases.

4.2 Jump Detection in Slope

Some simulation results of jump detection in the first-order derivative are presented in this part. We also use the example in Hall and Titterington (1992) which is shown in Figure 4.5. 512 observations $\{Y_i\}$ are obtained from $f(t_i) + \epsilon_i$ for equally spaced $t_i = i/512$, with iid errors from $N(0, \sigma^2)$ and $\sigma = 0.25$. $f(t) = 3t$ when $0 \leq t \leq 0.5$; $f(t) = 3 - 3t$ when $0.5 < t \leq 1$. It has one first-order jump at $t = 0.5$.

When $k = 121$, $\{\hat{\beta}_2^{(i)}\}$ and $\{\Delta_2^{(i)}\}$ are shown in Figure 4.6 (a) and (b) respectively. We performed our simulations with many k and n values. In each case, 1000 replications are done. Part of the results are presented in Figure 4.7.

Comparing Figure 4.4 with Figure 4.7, we find that the window width k should be chosen larger for slope change detection. The ratios of the "best" window widths to the sample sizes, $107/256 > 185/512 > 285/1024 > 469/2048$, are also decreasing as n increases. From Figure 4.7, it seems that k should be chosen as large as possible, but the boundary problem is more serious with larger k. Thus there is a trade-off on this issue. We plot the detected jump locations in 1000 replications with $k = 181$ and $n = 512$ in Figure 4.8. Comparing this gragh with Figure 4.3, we can see that it is more difficult to detect jumps in derivative than in the regression function itself.

4.3 Revisit the Sea-level Pressure Data

In Figure 1.1, we use $k = 15$ in both methods, which keeps the decreasing ratios of the "best" window widths to the sample sizes as we found in Figure 4.4. With this window size, values of the jump detection criterion are shown in Figure 4.9(b). A fitted polynomial regression function of order 4 has S.D. $\hat{\sigma} = 0.977$, leading to a jump threshold value $u_1 = 16.8$ for significance level 0.01. From the results, only $|\Delta_1^{(40)}| = |-18.077|$ (which corresponds to year 1960) exceeds u_1. Hence a jump appears to exist at year 1960 with significance level 0.01. The slope estimates $\{\hat{\beta}_1^{(i)}\}$ are shown in Figure 4.9(a). This plot reveals the jump around year 1960 very well.

5 Comparison with the Kernel-type Methods

5.1 Some Background

In this part we briefly introduce some kernel-type methods and compare their strengths and limitations to our algorithm. We hope it is helpful for practitioners to choose an appropriate method for a specific application.

The methods suggested by Müller (1992) and Qiu *et al.* (1991) assumed that there was only one jump point. Let

$$J(t) = \hat{m}_1(t) - \hat{m}_2(t) \tag{5.1}$$

and

$$|J(\hat{s})| = \max_{0 \le t \le 1} |J(t)|,$$

where $\hat{m}_1(t)$ and $\hat{m}_2(t)$ were two kernel estimators of the regression function $f(t)$ defined by a bandwidth h and two kernel functions $K_1(x)$ and $K_2(x)$ satisfying $K_1(x) = K_2(-x)$. Then $\hat{s}$ and $|J(\hat{s})|$ were defined as the estimators of the jump position and the corresponding jump magnitude, respectively. Qiu (1994) generalized these methods to the case with unknown number of jumps, but required that the jump magnitudes had a known lower bound.

Wu and Chu (1993) proposed a method to detect jumps when the number of jumps is unknown. Their proposal consisted of several steps. First, a series of hypothesis tests were performed for $H_0 : p = j \; vs \; H_a : p > j$ until an acceptance, where $j \geq 0$ and p was the true number of jump points. Then p maximizers $\{\hat{s}_j\}_{j=1}^{p}$ of $J(t)$ were defined as the jump position estimators. Finally, they used a rescaled $S(\hat{s}_j)$ to estimate the jump magnitude d_j for $j = 1, 2, \cdots, p$, where

$$S(t) = \hat{m}_3(t) - \hat{m}_4(t), \tag{5.2}$$

and $\hat{m}_3(t)$ and $\hat{m}_4(t)$ were two new kernel estimators of $f(t)$ defined by a bandwidth g and kernel functions $K_3(x)$ and $K_4(x)$.

A main limitation of the jump detection criteria (5.1) and (5.2) is that they did not take into account the derivatives to detect jumps in the regression function. Suppose that $f(t)$ is steep but continuous around some point t^*. Then both $S(t^*)$ and $J(t^*)$ could be large because of large derivative values. In other words, (5.1) and (5.2) did not exclude the continuous information from the jump information, which has been considered in our criterion $\Delta_1^{(i)}$ (Section 2). Müller (1992) used high-order kernels to detect jumps in derivatives. Our algorithm simply fits local polynomials with coefficients directly related to the derivatives of the regression function.

During the review process, we noticed some interesting properties of the jump detection criteria of the kernel-type methods ($J(t)$ in (5.1)) and the LS method ($\{\Delta_1^{(i)}\}$ in (2.1)). First, if t is a jump point, then $E(J(t)) = C_0$ and $Var(J(t)) = o(1)$ where C_0 is the jump magnitude. Second, $E(\Delta_1^{(i)}) = O(n/k) \to \infty$ when $n \to \infty$ and $Var(\Delta_1^{(i)}) = o(1)$. The convergence rate of $Var(J(t))$ is much faster than that of $Var(\Delta_1^{(i)})$. Based on this observation, $\Delta_1^{(i)}$ visually reveals the jumps better. This property is also helpful to select our threshold value, which could vary over a wide range without missing any real jumps. On the other hand, $\Delta_1^{(i)}$ is much noisier than $J(t)$. One referee pointed out that the coefficients of variation are of the same order in both situations. It should be an interesting future research topic to systematically compare these two kinds of methods.

5.2 An Example

Consider the regression function $f(t) = c(.5 - t) + I_{[0.5,1]}(t)$ having a single jump at $t = 0.5$ and slope c at continuous points. We choose $n = 512$ and $\sigma = 0.25$ as in Section 4. The regression function with $c = 4$ is displayed in Figure 5.1(a) along with its noisy version. We then apply the LS method and the method by Wu and Chu (1993) to detect the jump. Parameters in the LS procedure are chosen to be the same as those in Section 4. In the Wu and Chu procedure, the same kernel functions as those in their simulation examples are used. The bandwidth h is chosen 0.06 ($\approx 31/512$) which is compatible with the window size used in the LS procedure. The bandwidth g is chosen $2h$ which was suggested by Wu and Chu (1993).

A main purpose of this example is to show how the slope affects the jump detection in both methods. We let c vary among $3.0, 3.2, 3.4, 3.6, 3.8$ and 4.0. For each c value, the simulation is repeated 1000 times. In each simulation, estimators of the number of jumps (the true value is 1) by both methods are recorded. The Wu and Chu procedure gives a correct estimation if it rejects H_0 for $H_0 : p = 0$ vs $H_a : p > 0$ and accepts H_0 for $H_0 : p = 1$ vs $H_a : p > 1$ at the same time. We then count the number of correct estimations from 1000 replications for each method. The results are presented in Figure 5.1(b). It can be seen that the performance of the Wu and Chu procedure gets worse when c becomes larger ($f(t)$ is steeper at continuous points). The perfomance of our procedure, however, is quite stable. We plot $S(t_i)$ with $c = 4$ in Figure 5.1(c). It can be seen that $S(t_i)$ are relatively large at the continuous points because of large derivative values of $f(t)$. As a comparison, $\Delta_1^{(i)}$ (in plot (d)) of our procedure wave around 0 at the continuous points and have large values around the true jump point.

6 Concluding Remarks

We presented a jump detection algorithm with local polynomial fitting which is intuitively appealing and simple to use. Simulations show that it works well in practice.

Possible future research includes (a) determination of the value of m, which is not considered in this paper but may be important in applications; (b) selection of the window width k when the sample size is fixed, both from theoretical analysis and from simulation study; (c) generalization of this method to multivariate cases, especially the jump surface case which is directly related to many application areas such as image processing.

Acknowledgements The authors are grateful to the editor, the associate editor and two anonymous referees whose helpful suggestions lead to a great improvement of the presentation.

Appendix

A Properties of the Estimated LS Coefficients

The following two thoerems give some properties of the estimated LS coefficients used in Sections 2 and 3. Their proofs can be found in Qiu (1996).

Theorem A.1 For model (1.1)-(1.2), suppose that $m = 0$, $g(t)$, the continuous part of $f(t)$, has continuous first order derivative over (0,1) except on the jump points at which it has the first order right and left derivatives. Let the window width k satisfy the conditions that $\lim_{n\to\infty} k = \infty$ and $\lim_{n\to\infty} k/n = 0$. Then $\hat{\beta}_1^{(i)}$ in model (1.3) has the following properties. If there is no jump in $N(t_i)$, then

$$\hat{\beta}_1^{(i)} = g'(t_i) + O(\frac{n\sqrt{loglogk}}{k^{3/2}}), \quad a.s.$$

If there is a jump in $N(t_i)$ and the jump location is at $t_{i-\ell+r}, 0 \leq r \leq 2\ell$, then

$$\hat{\beta}_1^{(i)} = g'_+(t_i) + h_1(r)C_0 - \gamma(r)C_1 + O(\frac{n\sqrt{loglogk}}{k^{3/2}}), \quad a.s.,$$

where C_0 and C_1 are the jump magnitudes of $f(t)$ and its first order derivative at the jump location, $\gamma(r)$ is a positive function taking values between 0 and 1, $h_1(r) := \frac{6nr}{k(k+1)}(1 - \frac{r}{k-1})C_0$ and $g'_+(t_i) = g'(t_i)$ if $r \neq \ell$.

Remark A.1 The term $O(\frac{n\sqrt{\log\log k}}{k^{3/2}})$ in Theorem A.1 is due to noise in the model.

Theorem A.2 For model (1.1)-(1.2), suppose that $m = 1$, $g(t)$, the continuous part of $f'(t)$, has continuous first-order derivative over (0,1) except on the jump points at which it has the first order right and left derivatives. The window width k satisfies the conditions that $lim_{n\to\infty}k = \infty$ and $lim_{n\to\infty}k/n = 0$. Then $\hat{\beta}_2^{(i)}$ in model (1.3) has the following properties. If there is no jump in $N(t_i)$, then

$$\hat{\beta}_2^{(i)} = g'(t_i) + O(\frac{n^2\sqrt{loglogk}}{k^{5/2}}), \quad a.s.$$

If there is a jump in $N(t_i)$ and the jump location is at $t_{i-\ell+r}, 0 \leq r \leq 2\ell$, then

$$\hat{\beta}_2^{(i)} = g'_+(t_i) + h_3(r)C_1 - \gamma(r)C_2 + O(\frac{n^2\sqrt{loglogk}}{k^{5/2}}), \quad a.s.,$$

where C_1 and C_2 are the jump magnitudes of $f'(t)$ and its first order derivative, $\gamma(r)$ is a positive function taking values in [0,1],

$$h_3(r) := \frac{r(k-1-r)k[(k-1)(k-2)-3r(k-1-r)]}{12(ks_4-s_2^2)n^3},$$

$s_p = \sum_{j=i-\ell}^{i+\ell}(t_j-t_i)^p$, $p=2,4$, $g'_+(t_i)=g'(t_i)$ if $r\neq\ell$.

B Proof of Theorem 2.1

For design point $t_i \in (0,1)$, if $|t_i - s_j| > \frac{k+1}{2n}$ for any $j=1,2,\cdots,p$, then by Theorem A.1,

$$\Delta_1^{(i)} = O(\frac{n\sqrt{loglogk}}{k^{3/2}}), \quad a.s. \tag{B.1}$$

where $\{s_j, j=1,2,\cdots,p\}$ are the true jump positions as we defined in (1.2). On the other hand, if t_i is a jump point, then

$$\Delta_1^{(i)} \sim h_2(\ell)C_0 = O(\frac{n}{k}), \quad a.s. \tag{B.2}$$

By (2.3), the threshold value is

$$\begin{aligned} u_1 &= \hat{\sigma}Z_{\alpha_n/2}\frac{n}{k}\sqrt{\frac{6(5k-3)}{k^2-1}} \\ &= O(\frac{nZ_{\alpha_n/2}}{k^{3/2}}) \end{aligned} \tag{B.3}$$

Combining (B.1)-(B.3) and by the conditions stated in the theorem, the flagged design points $\{t_{i_j}, j=1,2,\cdots,n_1\}$ before the modification procedure satisfy

$$\{t_{i_j}, j=1,2,\cdots,n_1\} \subset \bigcup_{j=1}^{p} N(s_j) \tag{B.4}$$

where $N(s_j)$ is the neighborhood of s_j as we defined in Section 1.

After we use the modification procedure to delete some deceptive jump candidate points, we know that in each neighborhood $N(s_j)$ there is one and only one point of the final jump candidate set $\{b_j, j=1,2,\cdots,q_1\}$. Hence $\lim_{n\to\infty} q_1 = p$, $a.s.$ and $|b_j - s_j| = o(k/n)$, $a.s.$ If we choose $k=\log n$, then the conclusion of the theorem is obtained.

References

Besag, J., Green, P., Higdon, D., and Mengersen, K. (1995), "Bayesian computation and stochastic systems (with discussion)", *Statistical Science 10*, 3-66.

Eubank, R.L., and Speckman, P.L.(1994),"Nonparametric estimation of functions with jump discontinuities," IMS Lecture Notes, vol. 23, *Change-Point Problems* (E. Carlstein, H.G. Müller and D. Siegmund eds.), 130-144.

Gonzalez, R.C., and Woods, R.E. (1992), *Digital Image Processing*, Addison-Wesley Publishing Company, Inc.

Hall, P., and Titterington, M.(1992),"Edge-preserving and peak-preserving smoothing," *Technometrics 34,* 429-440.

Härdle, W.(1991), *Smoothing Techniques: with implementation in S*, New York: Springer-Verlag.

Hastie, T., and Tibshirani, R.(1987),"Generalized additive models: some applications," *Journal of the American Statistical Association 82,* 371-386.

Loader, C.R. (1994), "Change point estimation using nonparametric regression," AT&T Bell Laboratories.

McDonald, J.A., and Owen, A.B.(1986), "Smoothing with split linear fits," *Technometrics 28,* 195-208.

Müller, H.G.(1992),"Change-points in nonparametric regression analysis," *The Annals of Statistics 20,*737-761.

Qiu, P.(1991), "Estimation of a kind of jump regression functions," *Systems Science and Mathematical Sciences 4,* 1-13.

Qiu, P.(1994), "Estimation of the number of jumps of the jump regression functions," *Communications in Statistics-Theory and Methods 23,* 2141-2155.

Qiu, P.(1996), "Nonparametric estimation of discontinuous regression functions," Ph.D. Thesis, Department of Statistics, University of Wisconsin - Madison, Madison, WI 53706.

Qiu, P., Asano, Chi., and Li, X.(1991), "Estimation of jump regression functions," *Bulletin of Informatics and Cybernetics 24,* 197-212.

Qiu, P., and Bhandarkar, S.M. (1996), "An edge detection technique using local smoothing and statistical hypothesis testing," *Pattern Recognition Letters 17,* 849-872.

Qiu, P., and Yandell, B. (1997), "Jump detection in regression surfaces," *Journal of Computational and Graphical Statistics 6,* 332-354.

Shea, D.J., Worley, S.J., Stern, I.R., and Hoar, T.J. (1994),"An introduction to atmospheric and oceanographic data," NCAR/TN-404+IA, Climate and Global Dynamics Division, National Center For Atmospheric Research, Boulder, Colorado.

Shiau, J.H.(1987),"A note on MSE coverage intervals in a partial spline model," *Communications in Statistics-Theory and Methods 16,* 1851-1866.

Speckman, P.L.(1993),"Detection of change-points in nonparametric regression," Department of Statistics, University of Missouri, Columbia, MO 65211.

Stone, C.J.(1977),"Consistent nonparametric regression," *The Annals of Statistics 5,*595-620.

Wahba, G.(1986),"Partial spline modelling of the tropopause and other discontinuities," *Function Estimate, Contemporary Mathematics 59* (J.S. Marron eds.), 125-135.

Wu, J.S., and Chu, C.K.(1993),"Kernel type estimators of jump points and values of a regression function," *The Annals of Statistics 21*, 1545-1566.

Yin, Y.Q.(1988),"Detecting of the number, locations and magnitudes of jumps," *Communications in Statistics-Stochastic Models 4,* 445-455

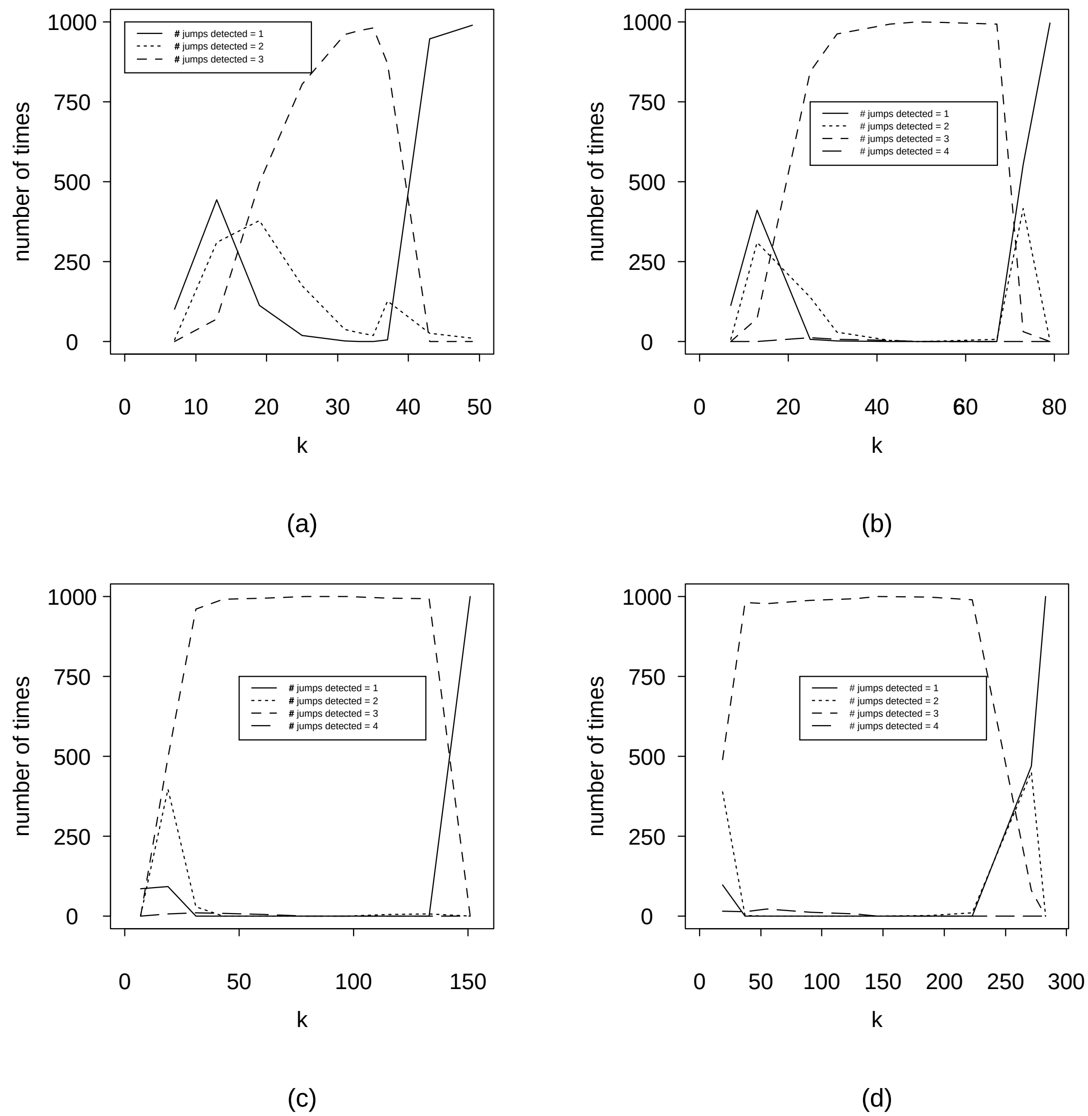

Figure 4.4: Distributions of the number of jumps detected by the zero-order jump detection algorithm in 1000 replications for several n and k values. (a) $n = 256$; (b) $n = 512$; (c) $n = 1024$; (d) $n = 2048$.

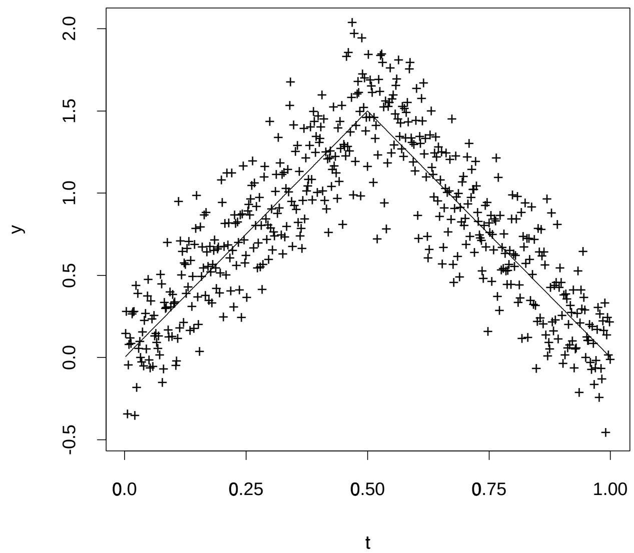

Figure 4.5: Hall and Titterington function f (solid lines) and observations (+).

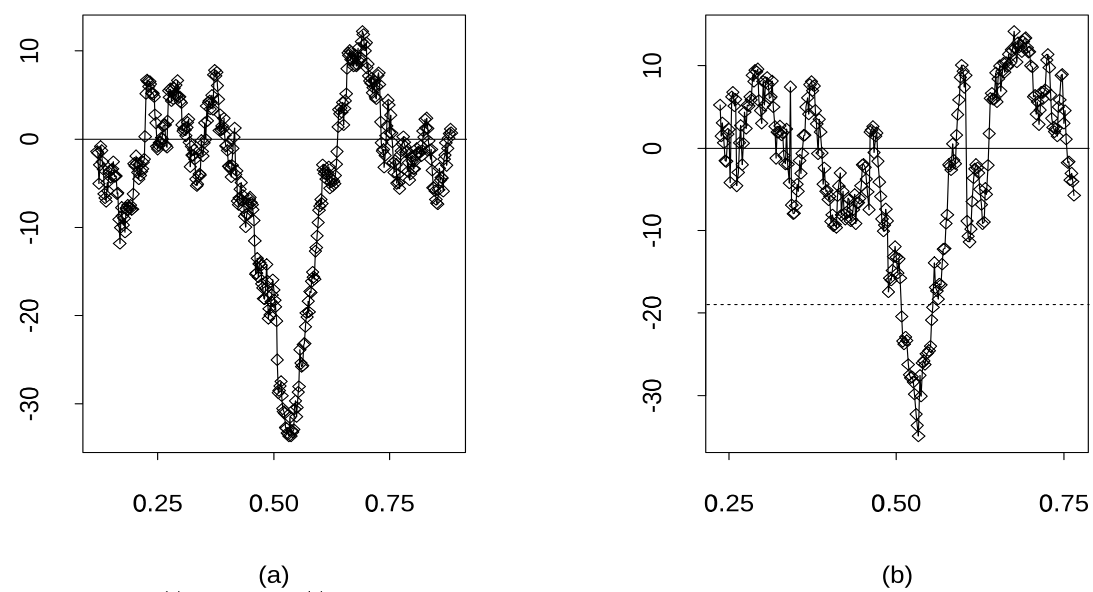

Figure 4.6: (a) $\{\hat{\beta}_2^{(i)}\}$ (b) $\{\Delta_2^{(i)}\}$ of the first-order jump detection algorithm. The dotted line in plot (b) indicates $(-)$ threshold value u_2 corresponding to $Z_{\alpha_n/2} = 3.5$.

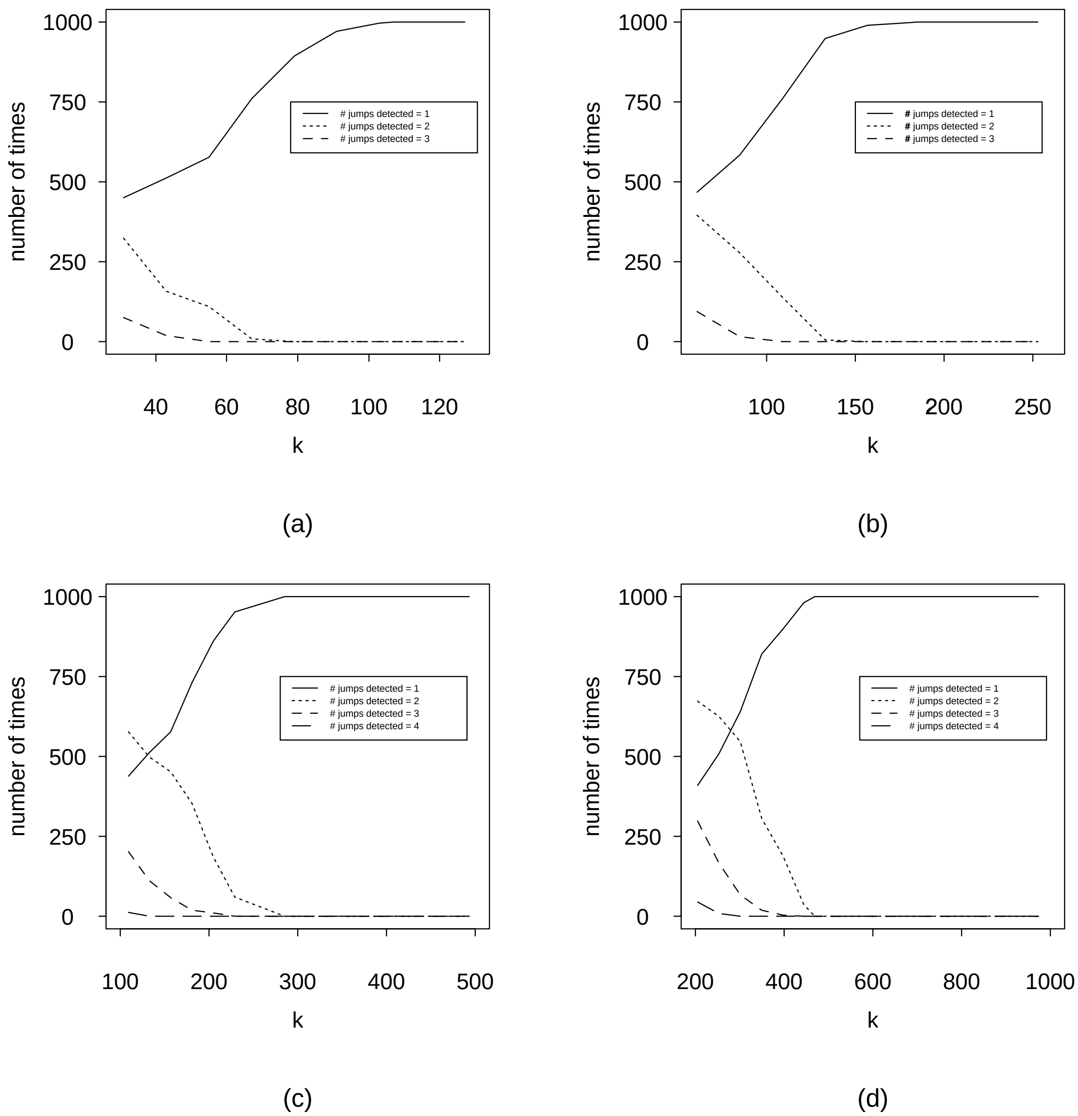

Figure 4.7: Distributions of the number of jumps detected by the first-order jump detection algorithm in 1000 replications for several k and n values. (a) $n = 256$; (b) $n = 512$; (c) $n = 1024$; (d) $n = 2048$.

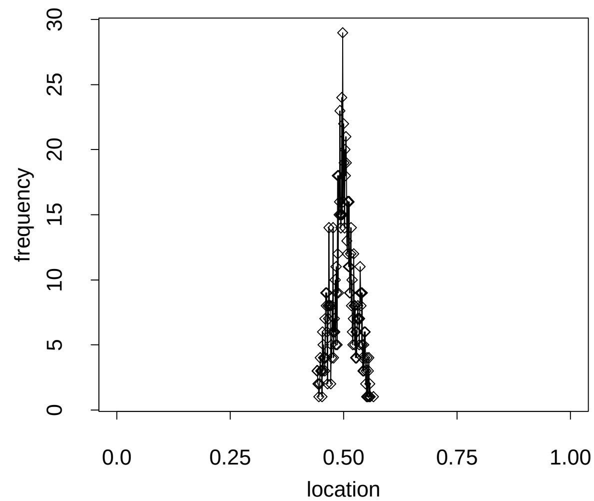

Figure 4.8: Frequency of detected jump locations by the first-order jump detection algorithm with $n = 512$ and $k = 181$ for 1000 replications.

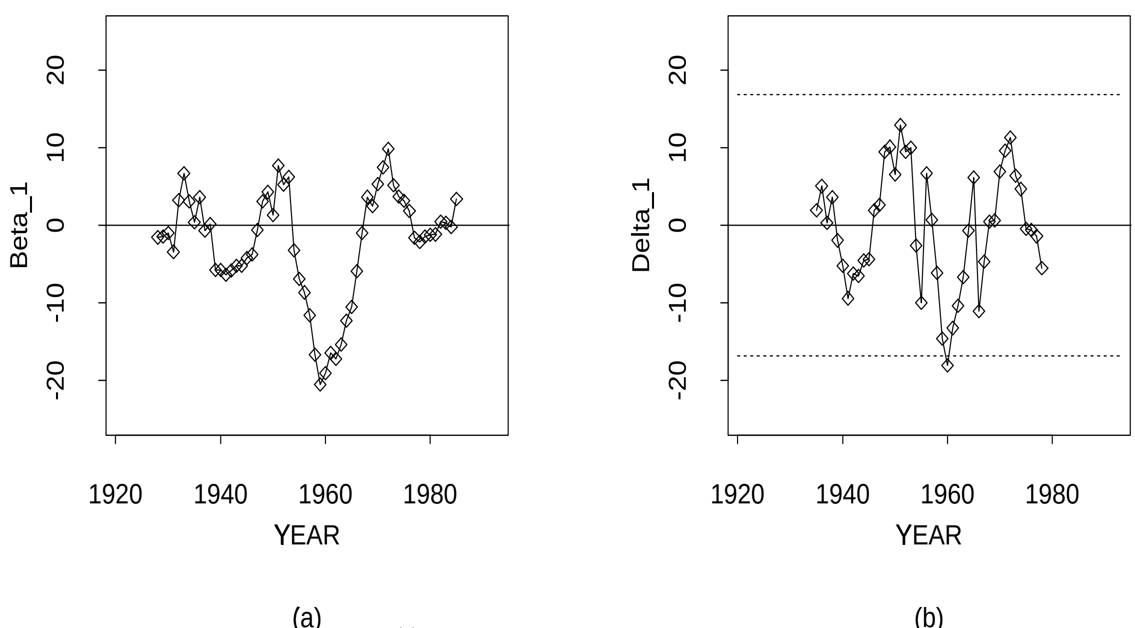

Figure 4.9: (a) Slope estimates $\{\hat{\beta}_1^{(i)}\}$ of the Bombay (India) sea-level pressure data; (b) values of the jump detection criterion.

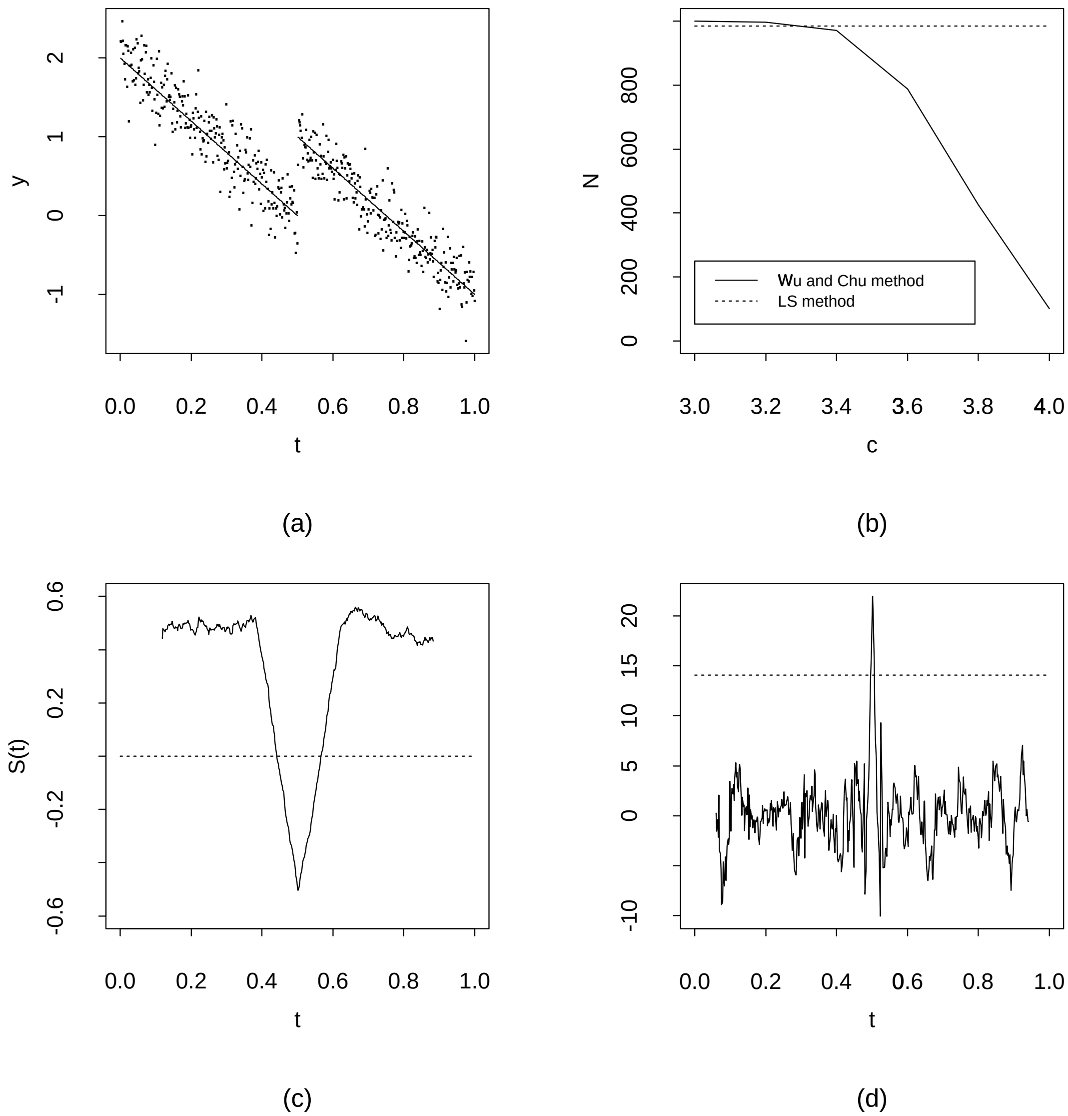

Figure 5.1: (a) Regression function and its noisy version. (b) Numbers of correct estimations (N) of the number of jumps out of 1000 replications when the slope c of the regression function changes from 3.0 to 4.0. (c) $\{S(t_i)\}$ of the Wu and Chu procedure. (d) $\{\Delta_1^{(i)}\}$ of the LS procedure. The dotted line in plot (c) indicates $S(t_i) = 0$. The dotted line in plot (d) denotes the threshold value of the LS procedure.